CHEMISTRY OF MATERIALS

COMMUNICATION

pubs.acs.org/cm

Novel Nanoporous Carbons from Well-Defined Poly(styrene-*co*-acrylonitrile)-Grafted Silica Nanoparticles

Dingcai Wu,[*,†,‡] Hongchen Dong,[†] Joanna Pietrasik,[§] Eun Kyung Kim,[†] Chin Ming Hui,[†] Mingjiang Zhong,[†] Mietek Jaroniec,[*,∥] Tomasz Kowalewski,[*,†] and Krzysztof Matyjaszewski[*,†]

[†]Department of Chemistry, Carnegie Mellon University, 4400 Fifth Avenue, Pittsburgh, Pennsylvania 15213, United States

[‡]Materials Science Institute, PCFM Laboratory, School of Chemistry and Chemical Engineering, Sun Yat-sen University, Guangzhou 510275, P.R. China

[§]Institute of Polymer and Dye Technology, Technical University of Lodz, Stefanowskiego 12/16, 90 924 Lodz, Poland

[∥]Department of Chemistry, Kent State University, Kent, Ohio 44242, United States

Supporting Information

KEYWORDS: nanoporous carbon, poly(styrene-*co*-acrylonitrile), SiO_2 nanoparticle, atom transfer radical polymerization (ATRP)

Nanoporous carbons are materials with a tunable set of physical and chemical characteristics, such as tailored pore shape and pore surface chemistry, high surface area and large pore volume, high electrical conductivity, and good thermal stability, making them suitable for numerous applications.[1] The most often explored applications include electrode materials for supercapacitors and rechargeable batteries, catalyst supports for fuel cells, adsorbents, chromatographic packing, and thermal insulators.[1] One of the most common and effective routes to prepare nanoporous carbon materials are template methods, including hard template and soft template methods. The hard template method often uses thermally stable inorganic materials, such as silica nanoparticles or ordered mesoporous silica SBA-15, while the soft template method usually employs thermally decomposable block copolymers to provide the tools for the formation of various types of nanopores.[1f,g,2] However, there are some drawbacks with both approaches. For example, the hard template method often involves incomplete filling of the pores and formation of a nonporous carbon as a result of deposition of carbon precursors on the external surface of the hard template.[2f] On the other hand, the soft counterpart usually deals with the high cost of some sacrificial soft templates.[1e,3]

Recently, our groups have successfully developed novel strategies for the preparation of nanoporous carbons, based on atom transfer radical polymerization (ATRP)[4] of acrylonitrile (AN)[4b,5] from initiation sites chemically bonded to hard templates including silica nanoparticles, ordered mesoporous silicas SBA-15 and FDU-1, and silica gel.[6] This approach provided a uniform filling of the template with polyacrylonitrile (PAN) and minimized the formation of nontemplated PAN, thus mitigating the formation of nontemplated carbon.

Carbon precursors have an important, or even a decisive, effect on the physical and chemical properties of the resulting carbon framework of the porous carbon materials.[7] For example, some carbon precursors, like PAN and pitch, usually create a carbon framework with a low microporosity, whereas others, like sucrose and specially cross-linked poly(styrene-*co*-acrylonitrile) (PSAN), generally impart a microporous nature to the carbon framework.[6b,7,8]

Scheme 1. Preparation Scheme of Nanoporous Carbon Material from Well-Defined Hairy PSAN-Grafted Nanoparticles

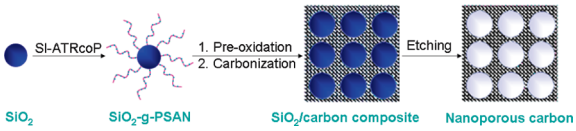

However, as compared to other template methods, the above ATRP-related synthesis methods have some disadvantages because of the limitations of suitable carbon precursors, and only PAN has been used so far.

In this communication, we report a novel type of nanoporous carbon with well-distributed uniform spherical mesopores as well as microporous carbon walls using well-defined PSAN-grafted SiO_2 nanoparticles (SiO_2-*g*-PSAN) as the carbon source and the template. As illustrated in Scheme 1, the overall synthesis procedure includes (1) conducting a surface-initiated atom transfer radical copolymerization (SI-ATRcoP)[9] of styrene (S) and AN from initiation sites chemically bonded to silica nanoparticles, thus obtaining SiO_2-*g*-PSAN; (2) preoxidation and carbonization of SiO_2-*g*-PSAN; and (3) silica removal from the resulting carbon/silica composite to form spherical mesopores within the carbon. During the preoxidation and carbonization treatments, the AN units undergo cross-linking, induced by oxygen in air, forming a continuous cross-linked polymer phase that is transformed into a carbon framework during carbonization. At the same time, the loss of thermally decomposable S units, as well as noncarbon elements and carbon-containing compounds in the above cross-linked polymer framework from AN units, leads to the formation of numerous micropores during preoxidation and carbonization. Furthermore, the as-obtained nanoporous carbon is in a macroscopic form of powder. It is different from its counterpart the SiO_2 nanoparticle-templated

Received: February 5, 2011
Revised: March 23, 2011
Published: April 01, 2011

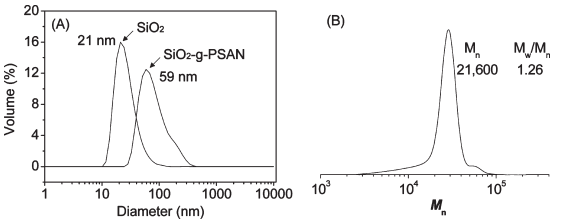

Figure 1. (A) DLS size distribution of SiO_2 nanoparticle and SiO_2-*g*-PSAN sample in THF. (B) GPC trace of the cleaved polymers from SiO_2-*g*-PSAN.

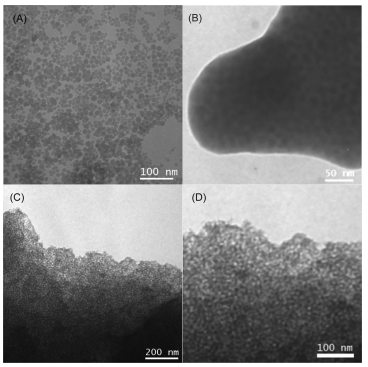

Figure 2. TEM images of (A) SiO_2 nanoparticle, (B) SiO_2-*g*-PSAN powder, and (C, D) nanoporous carbon.

nanoporous carbon film from SiO_2-*g*-PAN, making this type of ATRP-originated nanocarbons available for more applications, including but not limited to powdered nanomaterials. Potential applications include supercapacitor electrodes, catalyst supports for fuel cells, and coatings of solid-phase microextraction fibers. In addition, the use of PSAN as the carbon precursor provides component diversity and property tunability by ATRP, when compared to PAN. Thus, this new synthesis approach is expected to broaden the scope of ATRP-related nanocarbon materials.

According to the DLS result shown in Figure 1A, the hydrodynamic diameter of bare SiO_2 nanoparticles was ca. 21 nm, and their dispersity index was CV = 0.20, indicating a narrow size distribution. The diameter of the SiO_2 nanoparticles was also measured to be ~10 nm, according to the TEM image shown in Figure 2A. A smaller diameter of SiO_2 nanoparticles based on TEM than that from DLS can be ascribed to the fact that the hydrophilic state of nanoparticles would increase the diameter in suspension.[3] The SiO_2 nanoparticles were functionalized by reaction with 1-(chlorodimethylsilyl)propyl 2-bromoisobutyrate and then used for SI-ATRcoP of S and AN monomers, to prepare SiO_2-*g*-PSAN hybrid nanoparticles. The as-prepared SiO_2-*g*-PSAN were dissolved in THF, 1 mg/mL, and had a narrow and unimodal size distribution with hydrodynamic diameter of 59 nm by DLS (Figure 1A). PSAN was cleaved from the nanoparticles by etching SiO_2 with hydrofluoric acid (HF) and analyzed by GPC (Figure 1B). The cleaved PSAN had a narrow, unimodal molecular weight distribution (M_w/M_n = 1.26), with molecular weight M_n = 21 600, indicating a controlled surface-initiated ATRP. The S/AN molar ratio, the polymer content, and the grafting density in the hybrids were about 3/2, 64 wt %, and 0.12 chain/nm^2, respectively.

The SiO_2-*g*-PSAN nanoparticles were precipitated in the form of a macroscopic powder by addition to methanol. TEM images

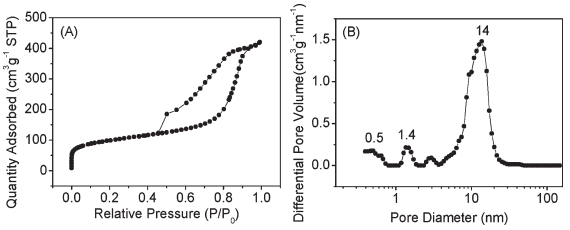

Figure 3. (A) N_2 adsorption−desorption isotherm and (B) DFT pore size distribution of nanoporous carbon.

showed the PSAN chains in the powder sample had undergone an intra/interparticle interlacing process during the precipitation step, as shown in Figure 2B and Supporting Information Figure S1. The tethered PSAN formed a continuous polymer phase with very evenly distributed SiO_2 nanoparticles because of the high uniformity of SiO_2-*g*-PSAN hybrid materials. The diameter of SiO_2 nanoparticles was estimated to be ca. 10 nm, and the polymer wall between the neighboring nanoparticles was about 8 nm, Figure 2B, although it is a little bit hard to accurately distinguish the border between the silica and the grafted polymer.

To obtain the nanoporous carbon, the polymer powder sample was preoxidized at 280 °C in an air flow and then carbonized at 700 °C in a N_2 flow, followed by removal of the hard template SiO_2 nanoparticle by HF. The AN units from the grafted PSAN chains underwent a intra/interchain cross-linking reaction with the help of air during the preoxidation treatment, thus forming a continuous cross-linked polymer phase. This facilitated the successful framework transformation from polymer to carbon during carbonization, confirmed by comparison of the TEM images shown in Figures 2B, 2C and 2D. The TEM analysis also demonstrated that the continuous phase shrank because of partial burnoff of the PSAN during preoxidation and carbonization, whose final yield was measured to be 25 wt %. The diameter of the resulting spherical mesopores in the as-prepared nanoporous carbon was very close to that of SiO_2 nanoparticles (~10 nm), indicating these nanoparticles efficiently played the template role. The obtained carbon wall was around 5 nm in thickness, obviously smaller than the corresponding polymer wall.

The pore structure of the nanoporous carbon was quantitatively analyzed by measurement of N_2 adsorption. The carbon sample showed type IV isotherms with a distinct hysteresis loop at relative pressure P/P_0 = 0.4−0.9, indicating the characteristics of a mesopore structure (Figure 3A)[1c,10], which was attributed to the SiO_2-templated spherical mesopores. The diameter of the mesopores, with a narrow size distribution, was calculated to be 14 nm by density functional theory (DFT) (Figure 3 B). Note that this diameter value is slightly different from that based from TEM image, most likely due to different characterization procedures. Meanwhile, as shown in Figure 3A, the amount of N_2 adsorption increased very sharply at low relative pressure, indicating the existence of numerous micropores. This can be ascribed to the burnoff of thermally decomposable S units, as well as noncarbon elements and carbon-containing compounds in the above cross-linked polymer framework from AN units during preoxidation and carbonization.[1e,3,8b] The sizes of the micropores are mainly centered at 0.5 and 1.4 nm according to the DFT calculation.

Brunauer−Emmett−Teller (BET) calculation showed that the nanoporous carbon had a BET surface area (S_{BET}) of 348 m^2 g^{-1}. The *t*-plot method demonstrated that the micropore surface area (S_{mic}) and external (i.e., mesopore) surface area (S_{mes}) were

dx.doi.org/10.1021/cm2003676 |*Chem. Mater.* 2011, 23, 2024–2026

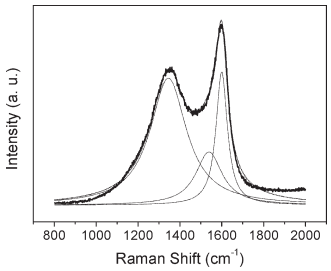

Figure 4. Raman spectrum of nanoporous carbon.

113 and 235 $m^2 g^{-1}$, respectively. The ratios of micropore (P_{mic}) and mesopore (P_{mes}) to the total surface area were calculated to be 32% and 68%, respectively, according to the following equations: $P_{mic} = (S_{mic}/S_{BET}) \times 100\%$ and $P_{mes} = 100\% - P_{mic}$. This means that the resulting carbon wall was highly microporous mainly due to the use of PSAN with high burnoff as carbon source. Its total pore volume (V_{total}) was measured to be 0.65 $cm^3 g^{-1}$ according to the adsorption amount at $P/P_0 = 0.99$.

The graphitic crystallite structure of nanoporous carbon was investigated by means of Raman spectroscopy. The Raman spectrum with a Lorentzian Fit Multipeaks analysis showed that nanoporous carbon had three bands around 1600, 1539, and 1345 cm^{-1} (Figure 4 and Supporting Information Table S1). The band around 1600 cm^{-1} is known as the G (graphitic) mode and is attributed to "in-plane" zone-center atomic vibrations of large graphite crystallites.[11] The band around 1530 cm^{-1}, denoted as A (amorphous) mode, was associated with amorphous sp^2-bonded forms of carbon arising from interstitial defects of nanoporous carbon.[12] The band around 1345 cm^{-1}, often called as D (disordered) mode, is attributed to the phonons near the Brillouin zone boundary active in small crystallites or on the boundaries of larger crystallites.[13] Furthermore, the microcrystalline planar crystal size L_a of nanoporous carbon can be calculated to be 1.4 nm (Supporting Information Table S1) using the empirical formula found by Tuinstra and Koeing ($L_a = 4.35 I_G/I_D$ (nm), where I_G and I_D are the integrated intensities of the G and D modes, respectively),[14] which indicated that the nanoporous carbon revealed a low graphitization degree.

To summarize, we have successfully developed a novel class of ATRP-related nanoporous carbons from hairy SiO_2-*g*-PSAN nanohybrids. It was demonstrated that spherical mesopores from the hard template SiO_2 nanoparticles were very evenly distributed within the final carbon nanomaterial that resulted from the well-defined structure of the grafted carbon precursor. Micropores were present within the continuous carbon wall because of the high burnoff of components in the PSAN, especially its thermally decomposable S unit. Carbon wall had small crystallite size. Currently, we are optimizing the nanostructure of this type of nanoporous carbon by tailoring composition and structures of the hairy SiO_2-*g*-PSAN, including molecular weight, S/AN ratio, grafting density, polymer/silica ratio, and SiO_2 particle size. This type of nanomaterial could find utility in a number of applications, such as supercapacitor electrodes, catalyst supports for fuel cell, adsorbents, nanomaterial templates, and so on.

■ ASSOCIATED CONTENT

Supporting Information. Experimental details (PDF). This material is available free of charge via the Internet at http://pubs.acs.org.

■ AUTHOR INFORMATION

Corresponding Author

*E-mail: km3b@andrew.cmu.edu (K.M.), tomek@andrew.cmu.edu (T.K.), jaroniec@kent.edu (M.J.), wudc@mail.sysu.edu.cn (D.W.).

■ ACKNOWLEDGMENT

We acknowledge financial support from National Science Foundation under Grant DMR 09-69301. D.W. acknowledges financial support from the project of NNSFC (50802116), SRFDP (200805581014), NSFGP (8451027501001421), and the Fundamental Research Funds for the Central Universities (09lgpy18). J.P. thanks the Foundation for Polish Science and Ministry of Science and Higher Education (Grant No. N508 3820 33) for the financial support.

■ REFERENCES

(1) (a) Su, D. S.; Schlögl, R. *ChemSusChem* **2010**, *3*, 136. (b) Dresselhaus, M. S. *Annu. Rev. Mater. Sci.* **1997**, *27*, 1. (c) Wu, D.; Fu, R.; Dresselhaus, M. S.; Dresselhaus, G. *Carbon* **2006**, *44*, 675. (d) Wu, D.; Fu, R.; Zhang, S.; Dresselhaus, M. S.; Dresselhaus, G. *Carbon* **2004**, *42*, 2033. (e) Zou, C.; Wu, D.; Li, M.; Zeng, Q.; Xu, F.; Huang, Z.; Fu, R. *J. Mater. Chem.* **2010**, *20*, 731. (f) Wan, Y.; Shi, Y.; Zhao, D. *Chem. Mater.* **2008**, *20*, 932. (g) Lee, J.; Kim, J.; Hyeon, T. *Adv. Mater.* **2006**, *18*, 2073.

(2) (a) Meng, Y.; Gu, D.; Zhang, F. Q.; Shi, Y. F.; Yang, H. F.; Li, Z.; Yu, C. Z.; Tu, B.; Zhao, D. Y. *Angew. Chem., Int. Ed.* **2005**, *44*, 7053. (b) Liang, C.; Dai, S. *J. Am. Chem. Soc.* **2006**, *128*, 5316. (c) Li, Z. J.; Jaroniec, M. *J. Am. Chem. Soc.* **2001**, *123*, 9208. (d) Wang, D.-W.; Li, F.; Liu, M.; Lu, G. Q.; Cheng, H.-M. *Angew. Chem., Int. Ed.* **2008**, *47*, 373. (e) Liang, Y. R.; Wu, D. C.; Fu, R. W. *Langmuir* **2009**, *25*, 7783. (f) Han, B. H.; Zhou, W. Z.; Sayari, A. *J. Am. Chem. Soc.* **2003**, *125*, 3444.

(3) Zeng, Q.; Wu, D.; Zou, C.; Xu, F.; Fu, R.; Li, Z.; Liang, Y.; Su, D. *Chem. Commun.* **2010**, *46*, 5927.

(4) (a) Wang, J.-S.; Matyjaszewski, K. *J. Am. Chem. Soc.* **1995**, *117*, 5614. (b) Matyjaszewski, K.; Xia, J. *Chem. Rev.* **2001**, *101*, 2921. (c) Matyjaszewski, K.; Tsarevsky, N. V. *Nat. Chem.* **2009**, *1*, 276. (d) Tsarevsky, N. V.; Matyjaszewski, K. *Chem. Rev.* **2007**, *107*, 2270. (e) Matyjaszewski, K.; Dong, H.; Jakubowski, W.; Pietrasik, J.; Kusumo, A. *Langmuir* **2007**, *23*, 4528.

(5) (a) Matyjaszewski, K.; Jo, S. M.; Paik, H. J.; Gaynor, S. G. *Macromolecules* **1997**, *30*, 6398. (b) Matyjaszewski, K.; Jo, S. M.; Paik, H. J.; Shipp, D. A. *Macromolecules* **1999**, *32*, 6431. (c) Kowalewski, T.; Tsarevsky, N. V.; Matyjaszewski, K. *J. Am. Chem. Soc.* **2002**, *124*, 10632.

(6) (a) Tang, C.; Bombalski, L.; Kruk, M.; Jaroniec, M.; Matyjaszewski, K.; Kowalewski, T. *Adv. Mater.* **2008**, *20*, 1516. (b) Kruk, M.; Dufour, B.; Celer, E. B.; Kowalewski, T.; Jaroniec, M.; Matyjaszewski, K. *J. Phys. Chem. B* **2005**, *109*, 9216.

(7) Li, S. Y.; Liang, Y. R.; Wu, D. C.; Fu, R. W. *Carbon* **2010**, *48*, 839.

(8) (a) Li, Z. J.; Jaroniec, M. *Carbon* **2001**, *39*, 2080. (b) Yang, X. Q.; Wu, D. C.; Fu, R. W. *Micro Nano Lett.* **2010**, *5*, 105.

(9) Tsarevsky, N. V.; Sarbu, T.; Gobelt, B.; Matyjaszewski, K. *Macromolecules* **2002**, *35*, 6142.

(10) Wu, D. C.; Chen, X.; Lu, S. H.; Liang, Y. R.; Xu, F.; Fu, R. W. *Microp. Mesop. Mater.* **2010**, *131*, 261.

(11) Li, G. B.; Lu, Z. H.; Huang, B. Y.; Wang, Z. X.; Huang, H.; Xue, R. J.; Chen, L. Q. *Solid State Ionics* **1996**, *89*, 327.

(12) Jawhari, T.; Roid, A.; Casado, J. *Carbon* **1995**, *33*, 1561.

(13) Baratta, G. A.; Arena, M. M.; Strazzulla, G.; Colangeli, L.; Mennella, V.; Bussoletti, E. *Nucl. Instrum. Methods Phys. Res., Sect. B* **1996**, *116*, 195.

(14) Tuinstra, F.; Koening, J. L. *J. Chem. Phys.* **1970**, *53*, 1126.